Mon. Not. R. Astron. Soc. **368,** L57–L61 (2006) doi:10.1111/j.1745-3933.2006.00157.x

# Excitation of g modes in Wolf–Rayet stars by a deep opacity bump

R. H. D. Townsend[1,2]★ and J. MacDonald[1]

[1]*Department of Physics & Astronomy, University of Delaware, Newark, DE 19716, USA*
[2]*Bartol Research Institute, University of Delaware, Newark, DE 19716, USA*

Accepted 2006 February 3. Received 2006 February 2; in original form 2006 January 7

**ABSTRACT**

We examine the stability of $\ell = 1$ and $\ell = 2$ g modes in a pair of nitrogen-rich Wolf–Rayet stellar models characterized by differing hydrogen abundances. We find that modes with intermediate radial orders are destabilized by a $\kappa$ mechanism operating on an opacity bump at an envelope temperature of $\log T \approx 6.25$. This 'deep opacity bump' is due primarily to L-shell bound–free transitions of iron. Periods of the unstable modes span ∼11–21 h in the model containing some hydrogen, and ∼3–12 h in the hydrogen-depleted model. Based on the latter finding, we suggest that self-excited g modes may be the source of the 9.8-h periodic variation of WR 123 recently reported by Lefèvre et al.

**Key words:** stars: individual: HD 177230 (WR 123) – stars: oscillations – stars: variables: other – stars: winds, outflows – stars: Wolf–Rayet.

## 1 INTRODUCTION

Of all of the differing excitation mechanisms responsible for free oscillations of stars [for a comprehensive review, see Unno et al. (1989) and references therein], none is more ubiquitous than the opacity, or '$\kappa$', mechanism. Put in simple terms, this mechanism works in layers of the envelope of a star where the opacity $\kappa$ increases in response to compression of the stellar material. Such an increase (initially produced, for instance, by stochastic perturbations to the equilibrium state) retards the escape of energy from the stellar core, with the trapped flux being deposited in the layer as heat. As Eddington (1926) discusses, the supply of additional heat during compression creates a Carnot-cycle heat engine capable of converting part of the outflowing radiant energy into mechanical energy. In tandem with a restoring force that returns the layer back toward its equilibrium state (pressure for p modes, buoyancy for g modes), the heat engine creates a condition of pulsational instability (overstability).

The role played by the $\kappa$ mechanism in the classical ($\delta$) Cephei pulsators was first identified by Zhevakin (1953). In these stars, the source of the instability is a peak in the opacity and its partial derivative $\kappa_T \equiv (\partial \ln \kappa / \partial \ln T)_\rho$ at an envelope temperature $\log T \approx 4.65$ where helium undergoes its second ionization. At lower luminosities, the same mechanism is primarily responsible for the RR Lyrae and $\delta$ Scuti classes of pulsating star [see Cox (1980) and references therein]. However, in the early-type $\beta$ Cephei stars and slowly pulsating (SPB) stars, the helium opacity bump is situated too close to the stellar surface to play any significant role in destabilizing pulsation modes.

In fact, the excitation mechanism responsible for these two classes of star remained a mystery until the advent of new opacities from the OPAL and Opacity Project (OP) initiatives (Rogers & Iglesias 1992; Seaton et al. 1994). The treatment of spin–orbit splitting in same M-shell transitions of iron and nickel, absent in previous calculations, introduced a new opacity peak at $\log T \approx 5.3$. Stability analyses by Cox et al. (1992), Dziembowski & Pamyatnykh (1993) and Dziembowski, Moskalik & Pamyatnykh (1993) revealed that this so-called 'iron bump' can destabilize p modes in $\beta$ Cephei stars and g modes in SPB stars. More recent investigations by Charpinet et al. (1997) and Fontaine et al. (2003) have inferred that the same iron bump can also drive the pulsation of the short-period (EC 14026) and long-period subdwarf B (sdB) stars.

In parallel with these developments, the new opacity data also impacted understanding of the pre-white dwarf GW Vir (pulsating PG 1159) stars. Starrfield et al. (1983, 1984) found that g modes in these objects could be $\kappa$-mechanism excited by an opacity bump around $\log T \approx 6.2$, arising from K-shell photoionization of carbon and oxygen; however, an almost pure C/O mixture was required for the instability to operate (Stanghellini, Cox & Starrfield 1991). This abundance restriction is relaxed when updated OPAL/OP data are adopted (see Gautschy, Althaus & Saio 2005, and references therein), owing to the appearance of extra opacity around $\log T \approx 6.3$. The origin of this additional opacity appears to be spin–orbit effects in L-shell bound–free transitions of iron (Rogers & Iglesias 1992).

From this brief survey of the literature, a natural question emerges. The iron bump in the OPAL/OP opacities leads to instability strips at both high masses ($\beta$ Cephei and SPB stars) and low masses (sdB stars). Given that the opacity bump at $\log T \sim 6$–$6.3$ drives pulsation in the low-mass GW Vir stars, is there by analogy a high-mass group of stars that also exhibit pulsation driven by this 'deep opacity bump' (DOB)? In order for the pulsation to be remain non-adiabatic around the driving zone, and therefore allow the $\kappa$-mechanism heat engine to operate, these putative stars must be exceedingly hot, with surface temperatures approaching $10^5$ K. In fact, these stars can be

★E-mail: rhdt@bartol.udel.edu

© 2006 The Authors. Journal compilation © 2006 RAS

recognized as massive, Population I, core helium burning Wolf–Rayet stars.

In this Letter, we conduct a preliminary stability analysis of a pair of model Wolf–Rayet stars, to evaluate the hypothesis that g modes can be excited in these stars by the DOB. We introduce the models in Section 2, and describe the stability analysis in Section 3. Our results are presented in Section 4, and then discussed and summarized in Section 5.

## 2 STELLAR MODELS

We evolve a star with an initial mass $M = 100\,\mathrm{M}_\odot$ and metallicity $Z = 0.02$ using a stellar structure code written by JM. The code is described in detail in Jimenez et al. (2004); the details pertinent to the present work are that (i) opacities are interpolated in the revised OPAL tables by Iglesias & Rogers (1996), (ii) the heavy-element mixture by Grevesse & Noels (1993) is assumed for the initial composition, and (iii) mass loss due to radiative driving is accounted for via a modified form of the formula given by Abbott (1982). The type 2 OPAL tables used by the code allow variation of the abundances of carbon and oxygen (in addition to hydrogen and helium), to reflect the effects of nucleosynthesis. Opacity changes due to a varying nitrogen abundance are simulated by adjusting the carbon and oxygen values passed to the opacity interpolation routine. Since the CNO elements are minor (and approximately interchangeable) opacity sources, this procedure should not introduce any significant error.

We track the evolution of the star off the main sequence, across to the red region of the Hertzsprung–Russell (HR) diagram, and back again to the blue. Two particular evolutionary stages are then selected as exemplars of nitrogen-enriched (WN) Wolf–Rayet stars. The 'WNL' (late-type) model is somewhat hydrogen-depleted, with a surface mass fraction $X_\mathrm{s} = 0.117$. The more evolved 'WNE' (early-type) model is completely devoid of hydrogen, but has yet to show any photospheric signature of carbon enrichment. Here, we use quotation marks around the labels of our models to emphasize that, in the same fashion as Langer et al. (1994), the designations 'early' and 'late' are to be understood in an evolutionary rather than a spectroscopic sense.

The fundamental parameters of both stellar models are summarized in Table 1. In Fig. 1, we plot the opacity and its derivative $\kappa_T$ as a function of temperature throughout the model envelopes. The DOB can be seen clearly as the peak around $\log T \approx 6.25$, while the iron bump also appears as a pronounced peak in the superficial layers around $\log T \approx 5.15$. By exploring the effects of modifying the heavy-element mixture, we have determined that the DOB is due primarily to iron, with minor contributions coming from nickel and the CNO elements.

## 3 STABILITY ANALYSIS

To analyse the stability of the Wolf–Rayet stellar models introduced above, we employ the BOOJUM non-radial, non-adiabatic pulsation code developed by RHDT. The current revision incorporates a few improvements over the baseline version described in Townsend (2005a,b). Most significantly, the roots of the characteristic equation

$$\mathcal{D}(\omega) = 0, \tag{1}$$

which define the stellar eigenfrequencies, are now first isolated using an approach similar to those suggested by Dziemblowski (1977) and Shibahashi & Osaki (1981). In this equation, $\omega$ is the pulsation frequency normalized by the inverse dynamical time-scale $\tau_\mathrm{dyn}^{-1} \equiv (GM_*/R_*^3)^{1/2}$, and $\mathcal{D}(\omega)$ is the discriminant function defined by equation (18) of Townsend (2005a).

The root isolation proceeds by dividing the complex-$\omega$ plane into many small rectangles, and evaluating for each one the contour integral

$$\mathcal{C} = \frac{1}{2\pi\mathrm{i}} \oint \frac{\mathrm{d}\mathcal{D}(\omega)}{\mathcal{D}(\omega)} \tag{2}$$

counterclockwise around the perimeter, via a recursively refined trapezoidal quadrature scheme. By Cauchy's theorem, $\mathcal{C}$ converges to the number of roots of the characteristic equation enclosed by the rectangle. Once a root is thus isolated, the frequency

$$\omega_\mathcal{C} = \frac{1}{2\pi\mathrm{i}\,\mathcal{C}} \oint \frac{\omega\,\mathrm{d}\mathcal{D}(\omega)}{\mathcal{D}(\omega)} \tag{3}$$

is used as the starting point in the secant root-finding algorithm implemented in BOOJUM. The $\mathcal{C}$ term in the denominator of this expression ensures that $\omega_0$ lies within the enclosing rectangle. Even though this term has an *analytical* value of unity, for a single enclosed root, its *numerical* value differs from unity because of the finite accuracy of our quadrature scheme.

This root isolation procedure is extremely useful in stars having high luminosity-to-mass ratios (such as Wolf–Rayet and GW Vir stars), because the pulsation tends to be so non-adiabatic (see Unno et al. 1989, their section 22.1) that solutions to the adiabatic pulsation equations furnish very poor starting points for the secant root finder. However, the contour integration often requires large numbers of quadrature points before $\mathcal{C}$ converges satisfactorily toward an integer

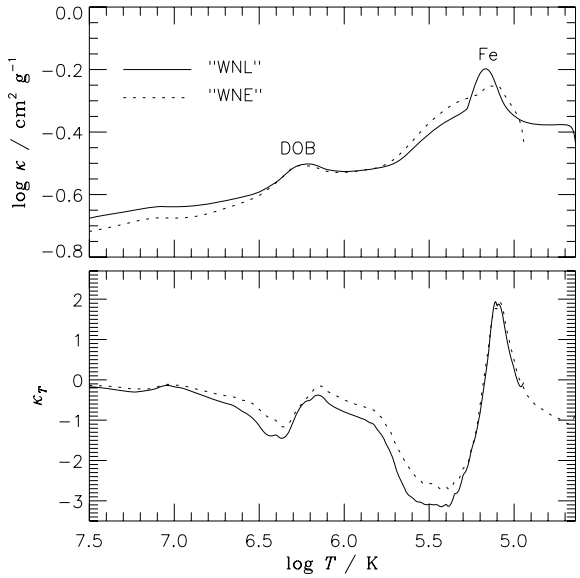


**Figure 1.** The opacity $\kappa$ (top) and its temperature derivative $\kappa_T \equiv (\partial \ln \kappa / \partial \ln T)_\rho$ (bottom), plotted as a function of envelope temperature for the 'WNE' (solid) and 'WNL' (dotted) stellar models. The labels indicate the location of the deep opacity bump (DOB) and iron opacity bump (Fe).

**Table 1.** Fundamental parameters of the stellar models introduced in Section 2. Note that the radii $R_*$ are for the hydrostatic core, and do not include the extended wind region containing the $\tau = 2/3$ photosphere (see Baschek, Scholz & Wehrse 1991).

| Model | age/Myr | $\log L_*/\mathrm{L}_\odot$ | $M_*/\mathrm{M}_\odot$ | $R_*/\mathrm{R}_\odot$ | $X_\mathrm{s}$ |
|---|---|---|---|---|---|
| 'WNL' | 3.57 | 5.77 | 20.6 | 10.3 | 0.117 |
| 'WNE' | 3.74 | 5.62 | 16.2 | 2.10 | 0.000 |

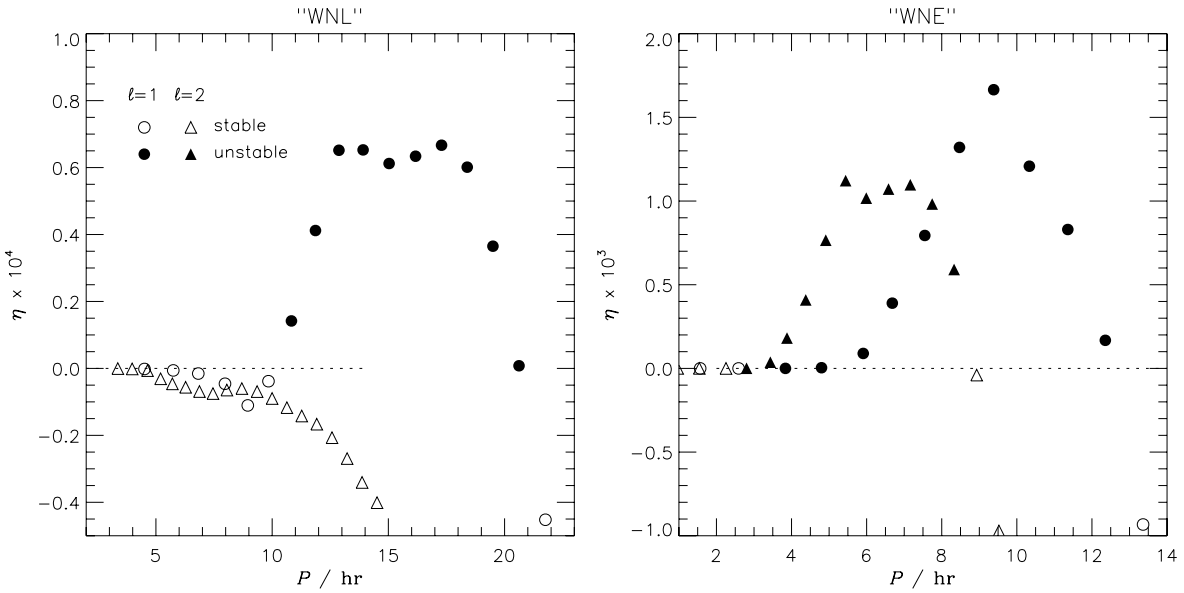


**Figure 2.** Normalized growth rates $\eta$ for the $\ell = 1$ (circles) and $\ell = 2$ (triangles) modes of the 'WNL' (left) and 'WNE' (right) stellar models, plotted as a function of pulsation period. The dotted line indicates the division between stable modes ($\eta < 0$; open symbols) and unstable modes ($\eta > 0$; filled symbols).

value. Hence, although adding robustness to the process of solving the non-adiabatic pulsation equations, root isolation is practical only when – as in the present work – a few individual stellar models are under study.

For the 'WNE' and 'WNL' models, we focus the stability analysis on g modes having harmonic degrees $\ell = 1$ and $\ell = 2$, searching for modes with radial orders $\tilde{n}$ between, approximately, 0 and $-25$. Here, $\tilde{n}$ is defined by Unno et al. (1989, their equation 17.5), within the generalization to the Cowling (1941) nomenclature introduced by Scuflaire (1974) and Osaki (1975). Negative values of $\tilde{n}$ typically correspond to g modes, but – as is often the case with more evolved stellar models – $\tilde{n}$ does not vary monotonically from one mode to the next, nor is it a unique index.

## 4 RESULTS

The results from the stability analysis are presented in Fig. 2, which plots the normalized growth rate $\eta \equiv -\Im(\omega)/\Re(\omega)$ of the modes found against their period $P$. Evidently, the 'WNE' model is unstable ($\eta > 0$) against $\ell = 1$ and $\ell = 2$ g modes having periods in the range ∼4–12 h and ∼3–8 h, respectively. Similar instability is seen in the 'WNL' model for $\ell = 1$ modes spanning the period range ∼11 − 21 h; however, the $\ell = 2$ modes of this model are all found to be stable.

To explore the origin of the instability, Fig. 3 plots the differential work for the $\ell = 1$ modes of each model that exhibit the largest growth rates. As discussed by Unno et al. (1989, their section 26.2), the $\kappa$ mechanism is operative wherever $\mathrm{d}\kappa_T/\mathrm{d}r > 0$. From Fig. 1, we see that this condition is met in the vicinity of the DOB, at a temperature $\log T \approx 6.3$. Since this location coincides with the sharp positive peak in the differential work of both models (indicating strong driving), we conclude that the unstable $\ell = 1$ and $\ell = 2$ modes are $\kappa$-mechanism excited by the DOB.

In Table 2, we summarize the properties of the unstable modes. The long-period limit of the instability arises because the pulsation interior to the opacity bump, at a temperature $\log T \approx 6.5$, becomes sufficiently non-adiabatic to activate strong radiative damping there.

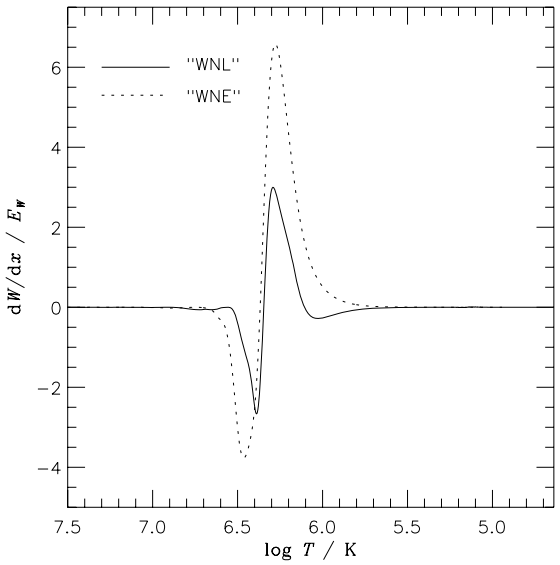


**Figure 3.** Differential work functions, plotted as a function of envelope temperature, for the $\ell = 1$ modes of the two stellar models having the largest growth rates. The differential is with respect to the dimensionless radius $x \equiv r/R_*$, and the work $W$ is expressed in units of the total energy of pulsation $E_W$.

Likewise, the short-period limit comes about because low-order modes exhibit a relative Lagrangian pressure perturbation $\delta p/p$ that is too small in the vicinity of the DOB to generate appreciable excitation [see Dziembowski et al. (1993) for a discussion of the role played by $\delta p/p$]. The $\ell = 2$ modes of the 'WNL' model are all stable for much the same reason; their $\delta p/p$ is peaked well exterior to the DOB, in a zone of inverted density stratification situated in the outer envelope at $\log T \approx 5.2$.

This inversion zone, which is present in both models, is responsible for a secondary family of unstable pulsation modes uncovered by BOOJUM. These modes, not shown in Fig. 3 because of our choice

© 2006 The Authors. Journal compilation © 2006 RAS, MNRAS **368,** L57–L61

**Table 2.** Properties of the unstable $\ell = 1$ and $\ell = 2$ g modes of the 'WNL' and 'WNE' stellar models. The subscripts $_{\min}$ and $_{\max}$ indicate the minimum and maximum values of the relevant quantities, respectively.

| Model | $\ell$ | $P_{\min}$/h | $P_{\max}$/h | $\tilde{n}_{\min}$ | $\tilde{n}_{\max}$ | $\eta_{\max}$ |
|---|---|---|---|---|---|---|
| 'WNL' | 1 | 10.8 | 20.6 | −20 | −10 | $6.67 \times 10^{-5}$ |
| 'WNL' | 2 | *No unstable modes* | | | | |
| 'WNE' | 1 | 3.83 | 12.4 | −14 | −4 | $1.67 \times 10^{-3}$ |
| 'WNE' | 2 | 2.81 | 8.34 | −15 | −5 | $1.12 \times 10^{-3}$ |

of ordinate range, are found for harmonic degrees $\ell = 1$ and $\ell = 2$, and are characterized by growth rates well in excess of $10^{-2}$ and energy densities strongly concentrated in the inversion zone. Following Saio, Baker & Gautschy (1998), we use this trapping property to classify the modes as non-radial strange modes. We note that the iron opacity bump is responsible for both the density inversions and the instability of the strange modes trapped within them. Since the strange modes are not related to the DOB, we shall not discuss them further.

## 5 DISCUSSION

In the preceding section, we demonstrate that low-degree, intermediate radial order g modes are unstable in a pair of stellar models representative of WN stars, due to a $\kappa$ mechanism operating on the DOB. This finding supports the central hypothesis of the paper advanced in Section 1, and likewise confirms WN stars as the high-mass cousins of GW Vir stars, exhibiting a relationship parallel to that between the high-mass $\beta$ Cephei and SPB stars, and the low-mass sdB pulsators.

However, there are caveats to our results. Beyond the various (reasonable) simplifications we adopt in constructing our stellar models (Section 2) and conducting the stability analysis (Section 3), we have neglected the effects of the strong, radiatively driven winds that are characteristic of all Wolf–Rayet stars. The stellar models incorporate only the evolutionary effects of wind-originated mass loss, and the stability analysis ignores the radial outflow at the outer boundary. As discussed by Cranmer (1996), an outflow can allow ordinarily trapped pulsation modes to propagate outward through the boundary. Townsend (2000) demonstrated that this leakage of wave energy can result in an appreciable damping of pulsations. If the unstable g modes found herein are to remain unstable, the rate of energy input from the $\kappa$ mechanism must exceed the damping due to leakage.

A thorough evaluation of this issue may have to await further theoretical advances in understanding how outflows influence pulsation. In the meantime, we discuss an observational development of particular relevance to the present work, one that poses some interesting questions regarding the role played by pulsation (whether leaking or not) in establishing structure and modulation in Wolf–Rayet winds. Although searches for *periodic* light variations in WN8 stars – the subtype most characterized by variability – have proven largely unsuccessful [see e.g. Marchenko et al. (1998), and references therein], recent *MOST* (*Microvariability and Oscillations of Stars*) observations of the WN8 star HD 177230 (WR 123) by Lefèvre et al. (2005) have detected an unambiguous 9.8-h periodic signal in the light curve of the star.

Pulsation appears a promising candidate for the origin of the variation of the star. Wolf–Rayet stars have been known for some time to be unstable toward strange modes (e.g. Glatzel, Kiriakidis & Fricke 1993); however, there is debate over whether such modes are compatible with the observations of WR 123. On the one hand, Lefèvre et al. (2005) themselves argue that the periods typical of strange modes, being of the order of the dynamical time-scale $\tau_{\rm dyn}$, are far too short to match the 9.8-h period detected by *MOST*. On the other hand, Dorfi, Gautschy & Saio (2006) reason that as a WN8 star WR 123 is expected to have a significantly larger radius, and hence longer strange mode periods, than the helium star models on which Lefèvre et al. (2005) based their conclusions. In support of their argument, Dorfi et al. (2006) present a WN8 model having $R_* = 15.4\,{\rm R}_\odot$ that exhibits unstable radial strange modes with periods of the order of a half day, seemingly compatible with the observations.

Here, there may be a problem. The large radii of the models studied by Dorfi et al. (2006) are, we believe, linked to the authors' *ab initio* assumption of an envelope hydrogen abundance $X = 0.35$. Although representative of many WN8 stars, this value is inappropriate to WR 123, which is well-known to be largely depleted of hydrogen ($X \lesssim 0.005$; see e.g. Crowther, Hillier & Smith 1995). It seems probable that the absence of hydrogen in the star is a consequence of it having already shed any residual hydrogen-rich envelope via wind mass loss. Accompanying the loss of this envelope should be a substantial reduction in the radius of the star, as can be seen by comparing our 'WNL' and 'WNE' models in Table 1.

Based on this reasoning, hydrogen-poor WR 123 may be characterized by an appreciably smaller radius than assumed by Dorfi et al. (2006), resulting once again in the period mismatch noted originally by Lefèvre et al. (2005). This leads us to advance g modes excited by the DOB as an alternative explanation for the variability of the star. As Fig. 2 illustrates, the 9.8-h period is covered by the unstable $\ell = 1$ g modes of the hydrogen-poor 'WNE' model. While we describe this model as 'early-type', we once again emphasize that the label is to be understood in an evolutionary rather than spectroscopic sense.

The detectable presence of g modes in WR 123 could offer unparalleled insights into the internal structure of the star; these modes penetrate down to the boundary of the convective core, and are therefore particularly well suited to asteroseismological analyses. However, it is unclear how best to proceed with the necessary initial step of testing our interpretation of the observations. Pulsation in g modes is often diagnosed through time-series monitoring of spectroscopic line profile variations (lpv); the predominantly horizontal velocity fields generated by these modes (e.g. Unno et al. 1989) tend to concentrate variability in the wings of line profiles. Unfortunately, this approach is not feasible in the case of Wolf–Rayet stars, because the supersonic wind washes out any lpv arising from (subsonic) pulsational velocity fields. It remains to be seen whether other approaches can be devised that are able to discriminate g modes from other potential sources of variability.

Beyond the specific case of WR 123, the discovery of a new class of Wolf–Rayet instability is of great interest in itself. Future investigation can now focus on exploring the characteristics and extent of the DOB instability in greater detail. Specific topics worthy of attention include establishing red and blue edges in the HR diagram, and determining the sensitivity of the instability against changes in input physics (e.g. elemental diffusion, mass-loss rates, etc.). As we have already noted, a proper treatment of pulsation at the outflowing outer boundary is also needed. An integral part of this treatment must be a better understanding of the reverse side of the pulsation–wind interaction: how can pulsation at the wind base lead to the modulations observed in Wolf–Rayet stars? Initial steps toward addressing this question were made by Cranmer & Owocki (1996), but there remains much work to be done.

**ACKNOWLEDGMENTS**

We thank Stan Owocki and Tony Moffat for their helpful remarks. RHDT acknowledges support from US NSF grant AST-0507581 and NASA grant NNG05GC36G. He is also grateful for the Bickle.

**REFERENCES**

Abbott D., 1982, ApJ, 259, 282
Baschek B., Scholz M., Wehrse R., 1991, A&A, 246, 374
Charpinet S., Fontaine G., Brassard P., Chayer P., Rogers F. J., Iglesias C. A., Dorman B., 1997, ApJ, 483, L123
Cowling T. G., 1941, MNRAS, 101, 367
Cox A. N., Morgan S. M., Rogers F. J., Iglesias C. A., 1992, ApJ, 393, 272
Cox J. P., 1980, Theory of Stellar Pulsation. Princeton Univ. Press, Princeton, NJ
Cranmer S. R., 1996, PhD thesis, University of Delaware
Cranmer S. R., Owocki S. P., 1996, ApJ, 462, 469
Crowther P. A., Hillier D. J., Smith L. J., 1995, A&A, 293, 403
Dorfi E. A., Gautschy A., Saio H., 2006, A&A, in press
Dziemblowski W., 1977, Acta Astron., 27, 95
Dziembowski W. A., Pamyatnykh A. A., 1993, MNRAS, 262, 204
Dziembowski W. A., Moskalik P., Pamyatnykh A. A., 1993, MNRAS, 265, 588
Eddington A. S., 1926, The Internal Constitution of the Stars. Cambridge Univ. Press, Cambridge
Fontaine G., Brassard P., Charpinet S., Green E. M., Chayer P., Billères M., Randall S. K., 2003, ApJ, 597, 518
Gautschy A., Althaus L. G., Saio H., 2005, A&A, 438, 1013
Glatzel W., Kiriakidis M., Fricke K. J., 1993, MNRAS, 262, L7
Grevesse N., Noels A., 1993, in Pratzos N., Vangioni-Flam E., Cassé M., eds, Origin and Evolution of the Elements. Cambridge Univ. Press, Cambridge, p. 15
Iglesias C. A., Rogers F. J., 1996, ApJ, 464, 943
Jimenez R., MacDonald J., Dunlop J. S., Padoan P., Peacock J. A., 2004, MNRAS, 349, 240
Langer N., Hamann W.-R., Lennon M., Najarro F., Pauldrach A. W. A., Puls J., 1994, A&A, 290, 819
Lefèvre L. et al., 2005, ApJ, 634, L109
Marchenko S. V., Moffat A. F. J., Eversberg T., Morel T., Hill G. M., Tovmassian G. H., Seggewiss W., 1998, MNRAS, 294, 642
Osaki J., 1975, PASJ, 27, 237
Rogers F. J., Iglesias C. A., 1992, ApJS, 79, 507
Saio H., Baker N. H., Gautschy A., 1998, MNRAS, 294, 622
Scuflaire R., 1974, A&A, 36, 107
Seaton M. J., Yan Y., Mihalas D., Pradhan A. K., 1994, MNRAS, 266, 805
Shibahashi H., Osaki Y., 1981, PASJ, 33, 427
Stanghellini L., Cox A. N., Starrfield S., 1991, ApJ, 383, 766
Starrfield S., Cox A. N., Kidman R. B., Pesnell W. D., 1984, ApJ, 281, 800
Starrfield S. G., Cox A. N., Hodson S. W., Pesnell W. D., 1983, ApJ, 268, L27
Townsend R. H. D., 2000, MNRAS, 319, 289
Townsend R. H. D., 2005a, MNRAS, 360, 465
Townsend R. H. D., 2005b, MNRAS, 364, 573
Unno W., Osaki Y., Ando H., Saio H., Shibahashi H., 1989, Nonradial Oscillations of Stars, 2nd edn. Univ. Tokyo Press, Tokyo
Zhevakin S., 1953, Russian Astron. J., 30, 161

This paper has been typeset from a TEX/LATEX file prepared by the author.

© 2006 The Authors. Journal compilation © 2006 RAS, MNRAS **368,** L57–L61